Virchows Archiv A Pathol Anat (1989) 414:187–198

Virchows Archiv A
Pathological Anatomy and Histopathology

An ultrastructural study of the hypertrophied human papillary muscle cell with special emphasis on specific staining patterns, mitochondrial projections and association between mitochondria and SR

Helge Dalen
Laboratory of Clinical Electron Microscopy, University of Bergen, 5021 Haukeland Hospital, Norway

Summary. Biopsy material of the hypertrophied human papillary muscle has been processed according to various electron microscopical techniques in order to study the mitochondrial ultrastructure and the association between mitochondria and sarcoplasmic reticulum (SR). *En bloc* staining with a Cu–Pb citrate solution resulted in specifically contrasted mitochondrial and sarcotubular membranes, characterized by numerous, discrete, electron-dense particles. The differences in staining patterns between the perinuclear mitochondria and their subsarcolemmal and interfibrillar counterparts suggest differences in chemical properties and/or metabolic activities. The selectively contrasted mitochondrial particles may represent a conglomorate of extrinisic and intrinisic respiratory enzymes and other membrane-associated proteins, while the majority of the electron-dense particles of the sarcotubular membrane may represent positively stained Ca^{2+}-pumps. Ultrastructural findings in the present study strongly indicate that the slender mitochondrial projections represent an initial stage in a process leading to the formation of large and pleomorphic mitochondria. Intimate contact between adjacent mitochondria as well as between mitochondria and SR are documented. In the contact regions some of the specifically contrasted particles of the adjacent membranes had fused with each other. It is suggested that these particles represent membrane-bound transport proteins providing a system for interorganelle exchanges of metabolites and/or ions.

Key words: Human heart – Papillary muscle – Hypertrophy – Mitochondria – Specific staining – Electron microscopy

Offprint requests to: H. Dalen

Introduction

Although an extensive body of literature has accumulated describing functional and ultrastructural alterations during the course of myocardial cell hypertrophy (see reviews by Ferrans 1984; Bugaisky and Zak 1986; Hamrell and Alpert 1986), information on the mitochondrial ultrastructure is incomplete.

In previous studies we have described various ultrastructural aspects of the hypertrophied human papillary muscle cells (Dalen et al. 1987a, b). In the present communication various electron microscopical techniques have been employed in order to characterize the finger-like mitochondrial processes and the peculiar contrasting patterns of the mitochondrial and sarcotubular membranes achieved after *en bloc* staining with a Cu–Pb citrate solution (Thiéry and Bergeron 1976). An attempt has also been made to obtain additional morphological evidence in support of the view that the outer mitochondrial membrane, at least in some regions, has established physical contact with the sarcoplasmic reticulum (Dalen et al. 1983, 1987b; Forbes and Sperelakis 1983).

Material and methods

Biopsies of the hypertrophied human papillary muscle were obtained from two adult patients subjected to mitral valve replacement. After surgical removal the tissue was immediately placed in ice-cold Hank's balanced salt solution, trimmed to small pieces and divided into four groups. The material of each group was prepared for ultrastructural studies according to one of the different methods described below.

Biopsy material designated for conventional transmission electron microscopy (TEM) was fixed overnight at 4° C in 2% glutaraldehyde and subsequently postfixed for 1 h in ice-cold 1% OsO_4. Both fixatives were made up in 0.1 M cacodylate buffer (pH 7.2) with 0.1 M sucrose, vehicle osmolality = 300 milliosmoles (Ericsson et al. 1978). After standard dehydration in ethanol, embedding in Epon 812 (Luft 1961) and polymeriza-

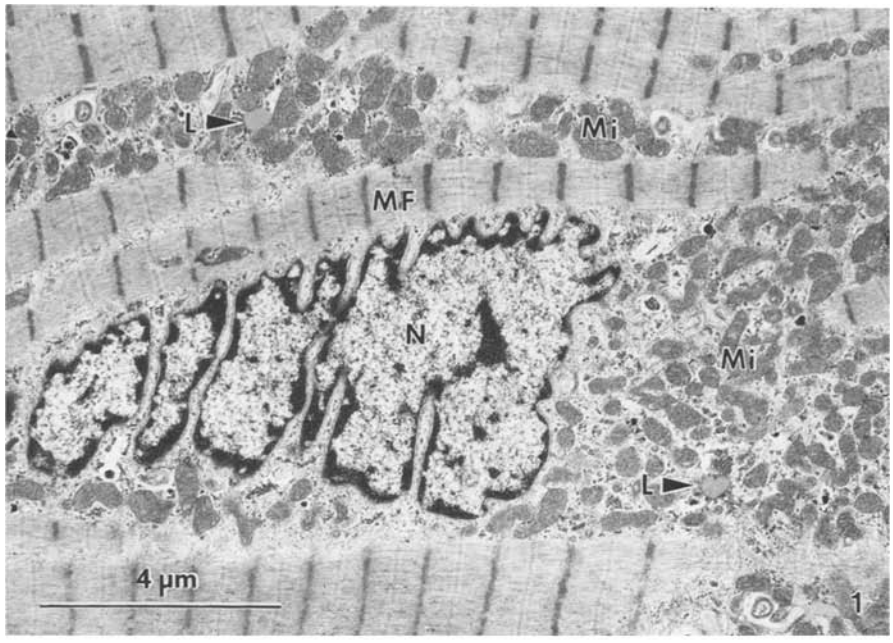

Fig. 1. TEM of a conventionally stained hypertrophied papillary muscle cell. Note the deeply invaginated nuclear envelope and the accumulations of mitochondria (*Mi*) in the nuclear pole sarcoplasm and interfibrillar space. *N*, nucleus. *MF*, myofibril. *L*, lipid droplets. × 8000

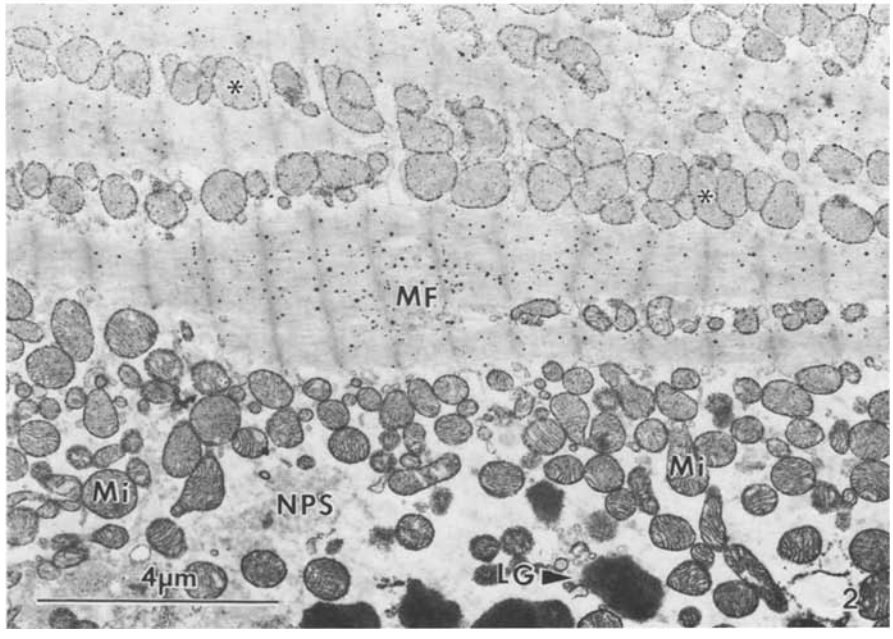

Fig. 2. A thin section of Cu–Pb impregnated tissue conventionally poststained with lead citrate and uranyl acetate. At low magnification the mitochondria (*Mi*) of the nuclear pole sarcoplasm (*NPS*) appear more densly contrasted than their counterparts of the interfibrillar space (*asterisks*). *MF*, myofibril; *LG*, lipofuscin granule. × 8000

tion, thick (1 µm) and thin sections were cut from the cured blocks on a Reichert ultramicrotome. For examination in the light microscope the thick sections were stained with toluidine blue, while the thin sections were collected on naked copper grids (300 mesh), conventionally contrasted with uranyl acetate (Watson 1958) and lead citrate (Reynolds 1963) and investigated in a Philips 300 TEM operated at 60 kV.

Another group of myocardial tissues, after fixation in 2% glutaraldehyde as above, was stained *en bloc* with a Cu–Pb citrate solution made up as described by Thiéry and Bergeron (1976). Postfixation for 24 h in ice-cold 1% cacodylate-buffered OsO_4 was followed by conventional dehydration, embedding in resin and polymerization. Thin and thick (0.5 or 1 µm) sections were picked up on 300 mesh copper grids. The thin sections with or without conventional staining with uranyl acetate and lead citrate were studied in the TEM at 60 kV, while the thick sections were examined without additonal contrasting in the TEM, using an accelerating voltage of 80 or 100 kV. In order to prepare stereo electron micrographs of the thick sections the goniometer stage was tilted plus or minus 6° from the zero position between two successive exposures.

Scanning electron microscopy (SEM) of intracellular structures was carried out on conventionally glutaraldehyde-fixed tissue, which had been embedded in paraffin and cryofractured at liquid N_2 temperature according to a procedure described by Dalen et al. (1978). After removal of the embeddment with xylol, the fractured material was critical point dried from CO_2 using acetone as a transitional solvent, mounted on specimen

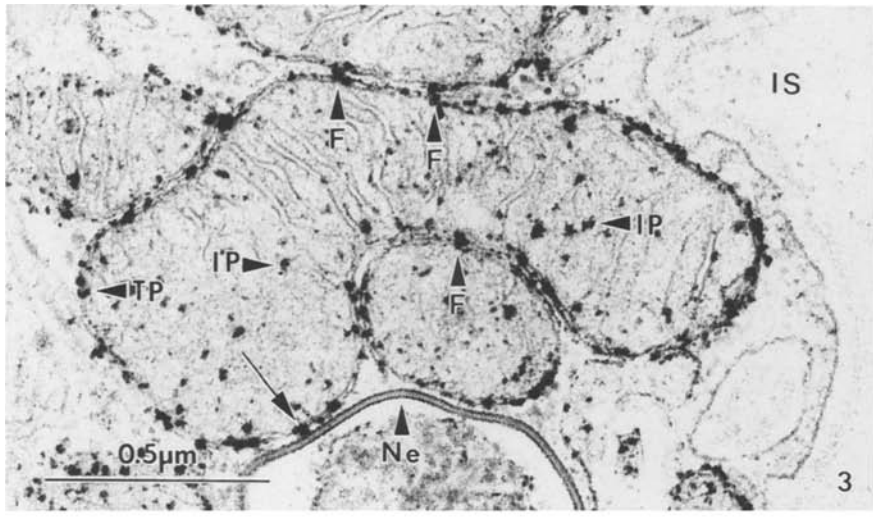

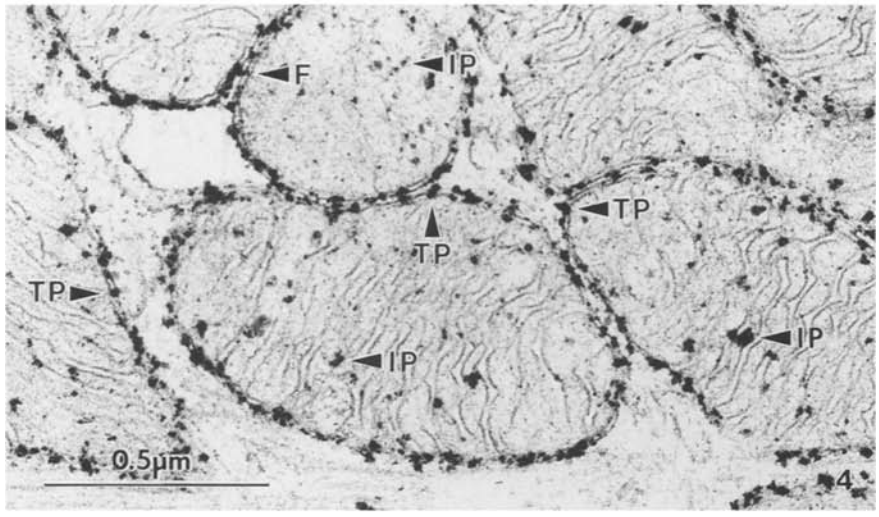

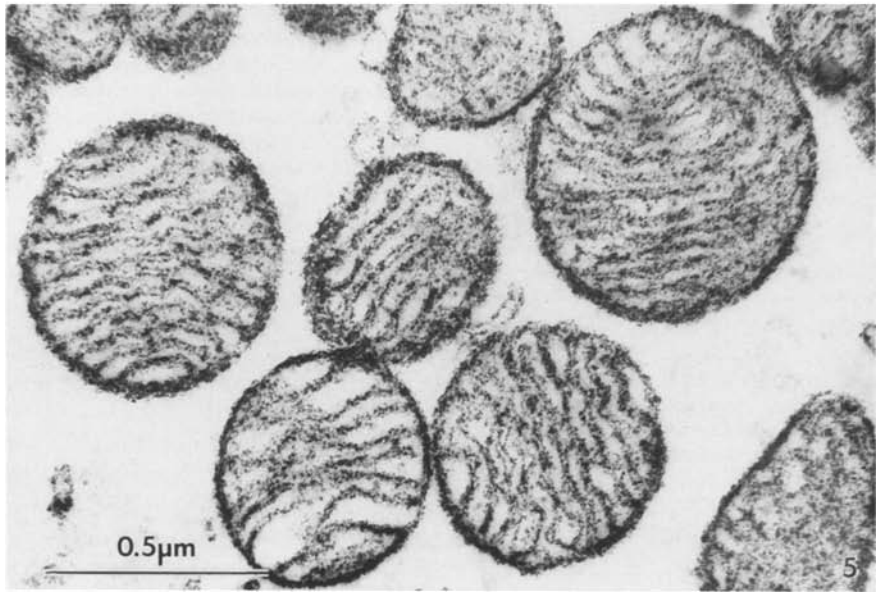

Figs. 3–5. Higher magnifications of the same material as depicted in Fig. 2 reveal mitochondrial populations with different staining patterns. The subsarcolemmal (**Fig. 3**) as well as the interfibrillar (**Fig. 4**) mitochondria are characterized by large and electron-dense transmembrane particles (*TP*) and by some specifically contrasted intramitochondrial particles (*IP*) of variable sizes. This pattern differs considerably from that of the perinuclear mitochondria (**Fig. 5**), where the *en bloc* staining procedure has resulted in numerous small and electron-dense particles located to the nuclear membranes and cristae. Note that some of the transmembrane particles of adjacent mitochondria have fused with each other (*F*) as well as made contact (*arrow*) with the nexus (*Ne*). *IS*, intercellular space. All micrographs ×60000

Fig. 6. Freeze fracture replica of mitochondria located in the nuclear pole sarcoplasm. The fractured mitochondrial membranes (*asterisks*) exhibit numerous intramembrane/transmembrane proteins. Note the particulated bands located in the mitochondrial matrix representing transversly fractured cristae (*arrowheads*). × 60000

holders, sputter-coated with gold (Echlin 1975), and viewed in a Philips 500 SEM operated at 25 kV. Stereo-pair micrographs were obtained by tilting the goniometer stage 10° between two successive exposures.

Freeze fracture replicas were processed from myocardial tissue fixed for 30 min at 4° C in 2% glutaraldehyde followed by 30 min impregnation with 30% glycerol. Both the fixative and the cryoprotectant were made up in the same vehicle as described above. The material was mounted on gold holders, frozen in melting Freon 22, and freeze fractured at −100° C. Replication with platinum-carbon was carried out according to standard procedures in a Balzer's freeze fracture apparatus equipped with electron guns. The replicas were cleaned with a sodium hypochlorite solution, collected on formvar coated grids and viewed in the TEM at 80 kV.

Results

Thin sections of the hypertrophied papillary muscle cells displayed a variable number of mitochondria accumulated in the interfibrillary space and in the perinuclear region (Fig. 1).

En bloc staining with a Pb–Cu citrate solution resulted in specifically contrasted mitochondria (Figs. 2–5). At low magnification the mitochondria of the nuclear pole sarcoplasm appeared considerably darker than their interfibrillar counterparts (Fig. 2). Higher magnification revealed that this phenomenon was due to different staining pat-

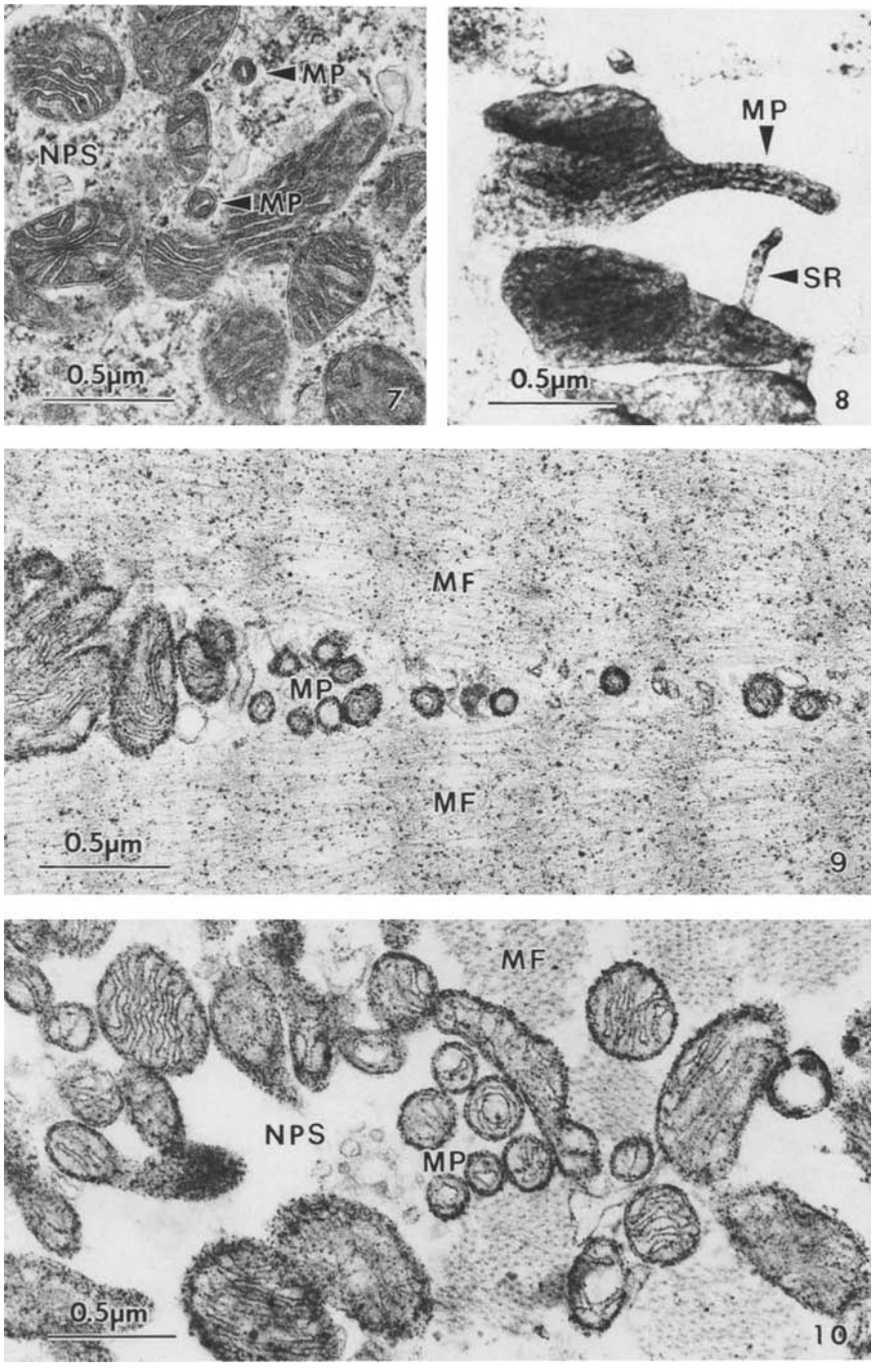

Fig. 7–10. Cross (**Figs. 7, 9–10**) and longitudinal (**Fig. 8**) sections of mitochondrial processes (MP) as they appear in thin (**Figs. 7, 9–10**) and in 1 μm thick (**Fig. 8**) sections of conventionally processed (**Fig. 7**) and Cu–Pb impregnated (**Figs. 8–10**) myocardial cells. In some cases (**Fig. 9**) the mitochondrial projections have penetrated the narrow clefts between adjacent myofibrils (*MF*). The cristae, which are oriented parallel to the long axis of the mitochondrial extension (**Fig. 8**), display various configurations when cut transversly. Some of the larger projections seen in **Fig. 10** may represent interconnecting mitochiondrial processes. NPS, nuclear pole sarcoplasm. SR, sacroplasmic reticulum. All micrographs × 35000

terns. The interfibrillar as well as the subsarcolemmal mitochondria exhibited some large and electron-dense particles associated with the surrounding mitochondrial membranes as well as scattered throughout the mitochondrial interior (Figs. 3–4). The specifically stained particles of the perinuclear mitochondria, however, were considerably smaller and were confined to the outer and inner mitochondrial membranes, including the cristae, where they occured in large numbers (Fig. 5). Similar particulated structures were also revealed in freeze fractured mitochondria (Fig. 6). The specifically stained transmembrane particles commonly were seen to have fused with their counterparts of adjacent mitochondria as well as to have made contacts with the nexus (Figs. 3–4).

Peculiar finger-like processes extending beyond the main mitochondrial body were frequently ob-

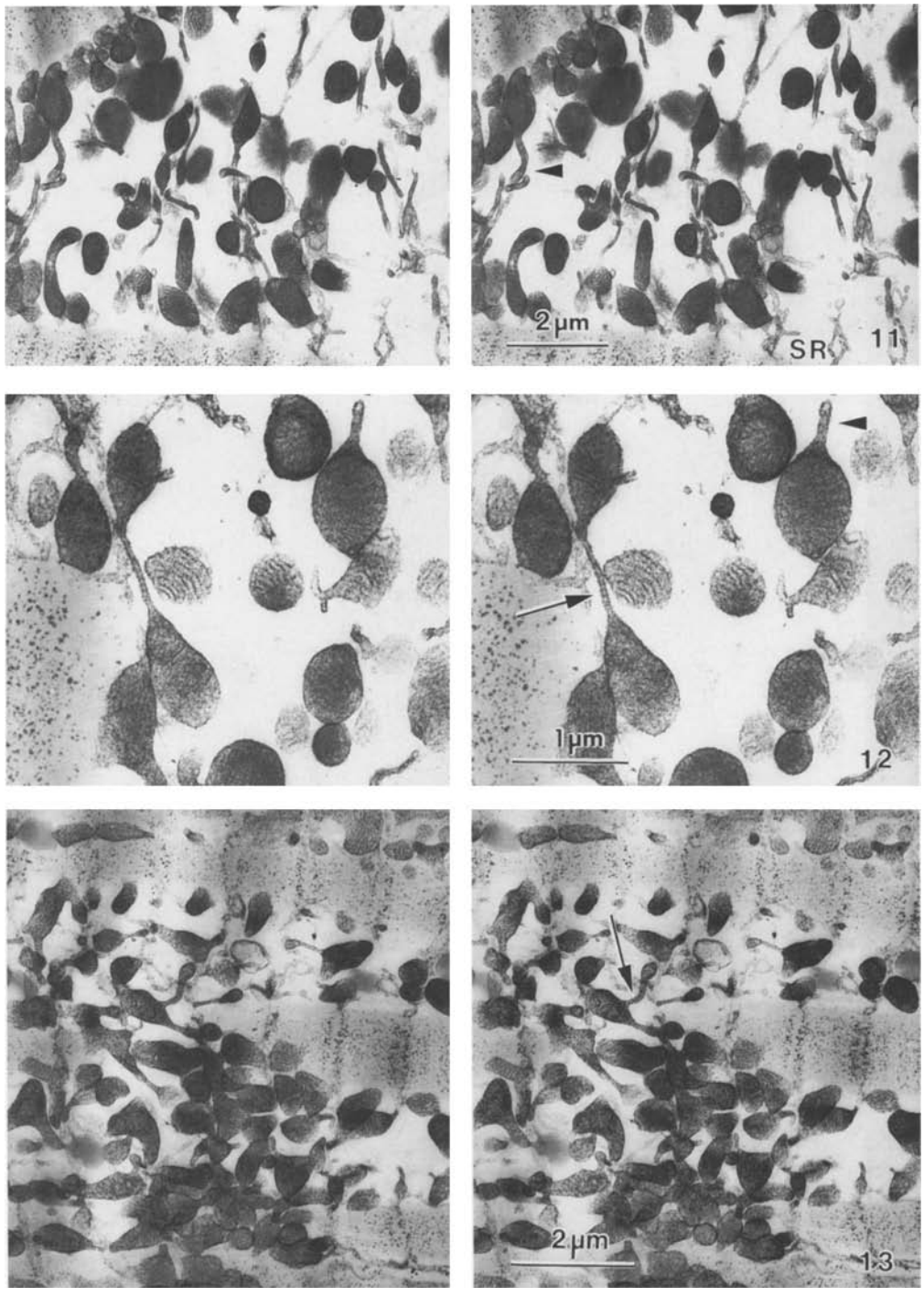

Figs. 11–13. Stereo-pair (12° tilt) electron micrographs of 1 µm thick sections of *en bloc* stained tissue demonstrating numerous mitochondrial projections (**Figs. 11–12**), a dumbbell-shaped mitochondrion (**Fig. 12**) and pleomorphic mitochondria (**Fig. 13**). Note that the sarcotubular membranes (SR) differ from the mitochondrial extensions (*arrowheads*) in that they are less electron-dense, and that slender mitochondrial interconnections (*arrows*) are observed in dumbbell-shaped and pleomorphic mitochondria. **Fig. 11**, ×7500; **Fig. 12**, 17000; **Fig. 13**, ×9000

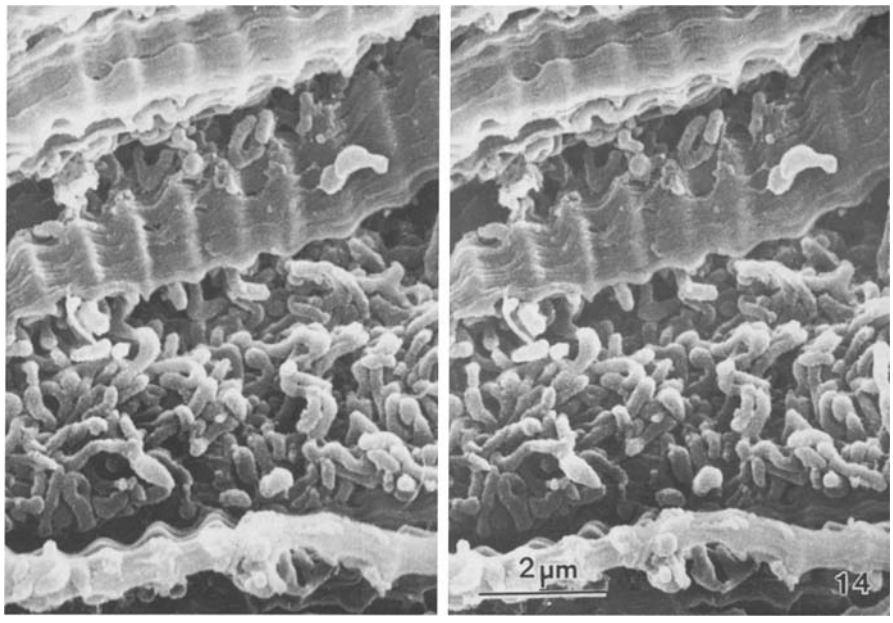

Fig. 14. An example of accumulated pleomorphic mitochondria as they appear in a stereo-pair (10° tilt) scanning electron micrograph of a cryofractured papillary muscle cell. ×8500

served in those hypertrophied myofibers in which the mitochondria had not reached the state of densly packing (Figs. 7–12). Thick sections of Cu–Pb impregnated material revealed that the cristae within these processes were continous with the cristae of the main mitochondrial body, and that they were oriented parallel to the long axis of the projections (Fig. 8). When cut transversly, the mitochondrial extensions appeared as circular profiles displaying various cristal configurations (Figs. 7, 9–10). The slender processes, which were oriented perpendicular to (Fig. 9) as well as parallel to (Fig. 10) the long axis of the myofibrils, penetrated the narrow interfibrillar clefts (Fig. 9).

The pleomorphic nature of the mitochondria was best illustrated by stereo transmission (Fig. 11–13) and scanning (Fig. 14) electron micrographs of Cu–Pb impregnated tissue and cryofractured material, respectively. The bulky mitochondrial bodies of branched mitochondria were seen frequently to be interconnected by slender processes (Fig. 13).

Sarcotubular membranes also exhibited specific staining properties which facilitated ultrastructural studies of the SR-mitochondrial relationship (Figs. 15–19). TEM micrographs of thick sections strongly suggested an intimate contact between the SR and the outer mitochondrial membrane in all regions of the myofiber (Figs. 15–17). High magnification of thin sections revealed physical contact between the electron-dense particles of the two membranes (Figs. 18–19). Indeed, in some places the electron-dense particles of the two membranes had fused with each other. The three-dimensional relationship between the SR and the mitochondria was illustrated with stereo transmission electron micrographs of Cu–Pb impregnated tissue (Fig. 20) as well as with mono and stereo-pair scanning electron micrographs of cryofractured material (Figs. 21–22). Strands of intermediary SR interconnected the mitochondria with the juxtafibrillar SR preferentially at the sites of the Z-band and M-band (Fig. 22).

Discussion

Specific contrasting of intracellular membranes has been achieved by *en bloc* staining with a Cu–Pb citrate solution (Thiéry and Bergeron 1976). This method has been used successfully in myocardial cell research for studying the subcellular organization of mitochondria and SR in tissue obtained from the left ventricle of healthy rats (Segretain et al. 1981) and from the hypertrophied human papillary muscle (Dalen et al. 1987b). While the cytochemical mechanism for this *en bloc* staining method has not been clarified, it has been suggested that the metal ions of the staining solution bind specifically to carboxyl groups of membrane-associated proteins (Dalen et al. 1987b).

The observation here that the specific contrasting pattern of the perinuclear mitochondria differs considerably from that of their interfibrillar and subsarcolemmal counterparts may reflect differences in chemical properties and/or in metabolic

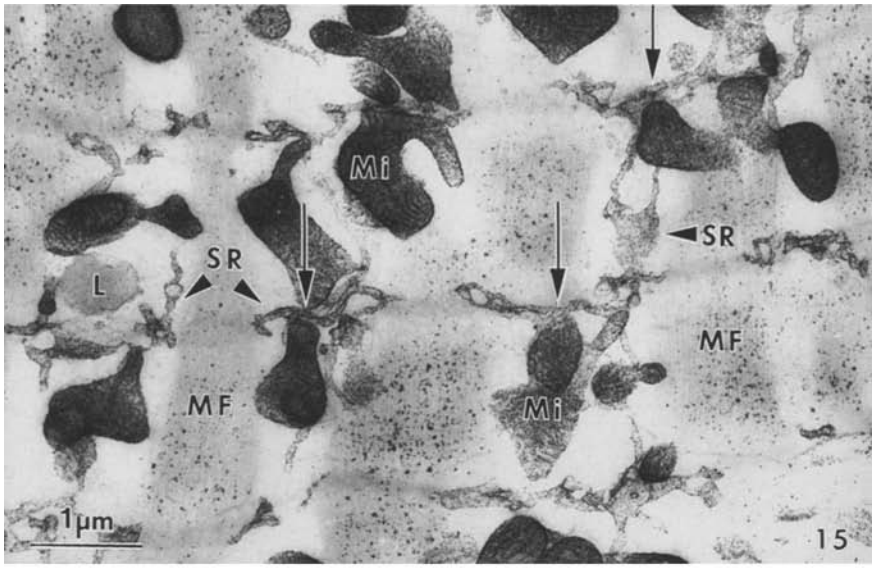

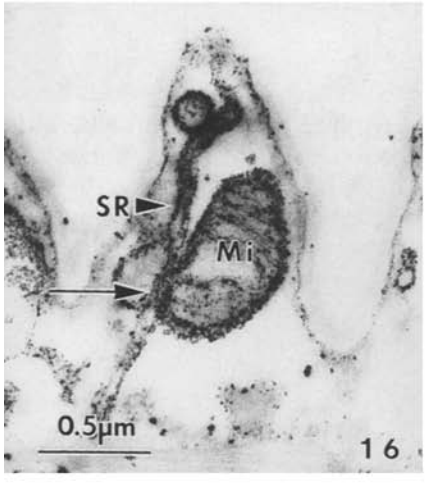

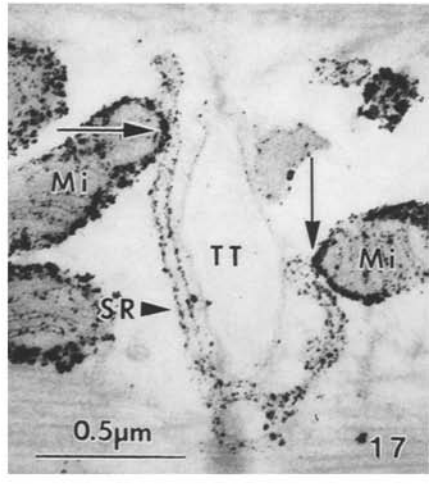

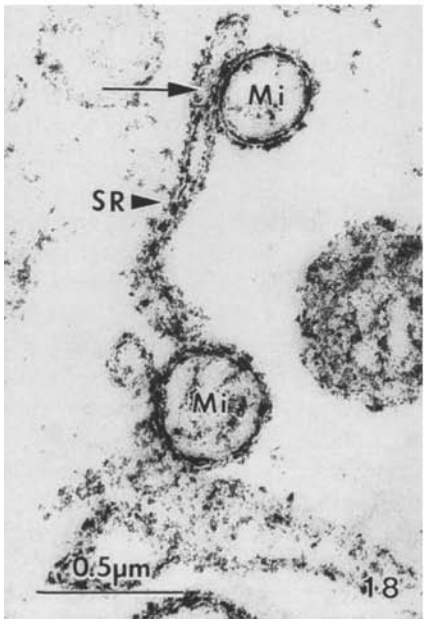

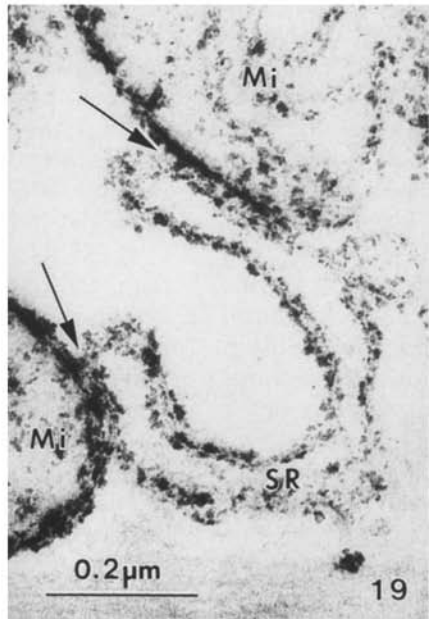

Fig. 15. A transmission electron micrograph of a thick (1 μm) section of Cu–Pb impregnated material. Note the close relationship (*arrows*) between mitochondria (*Mi*) and sarcoplasmic reticulum (*SR*). *MF*, myofibrils. *L*, lipid droplet. ×15000

Figs. 16–17. Thick sections (0.5 μm) of specifically contrasted tissue displaying the close contact (*arrows*) between mitochondria (*Mi*) and SR as it is revealed in the sarcolemmal fold (**Fig. 16**) and in the interfibrillar space (**Fig. 17**). *TT*, transfer tubule. **Fig. 16**, ×30000; **Fig. 17**, ×40000

Figs. 18–19. The physical contact (*arrows*) between SR and mitochondria (*Mi*) as it is demonstrated in thin sections of the Cu–Pb impregnated myocardial cells. Note that some of the electron- dense sarcotubular particles in the contact region have fused with their mitochondrial counterparts. **Fig. 18**, ×40000; **Fig. 19**, ×100000

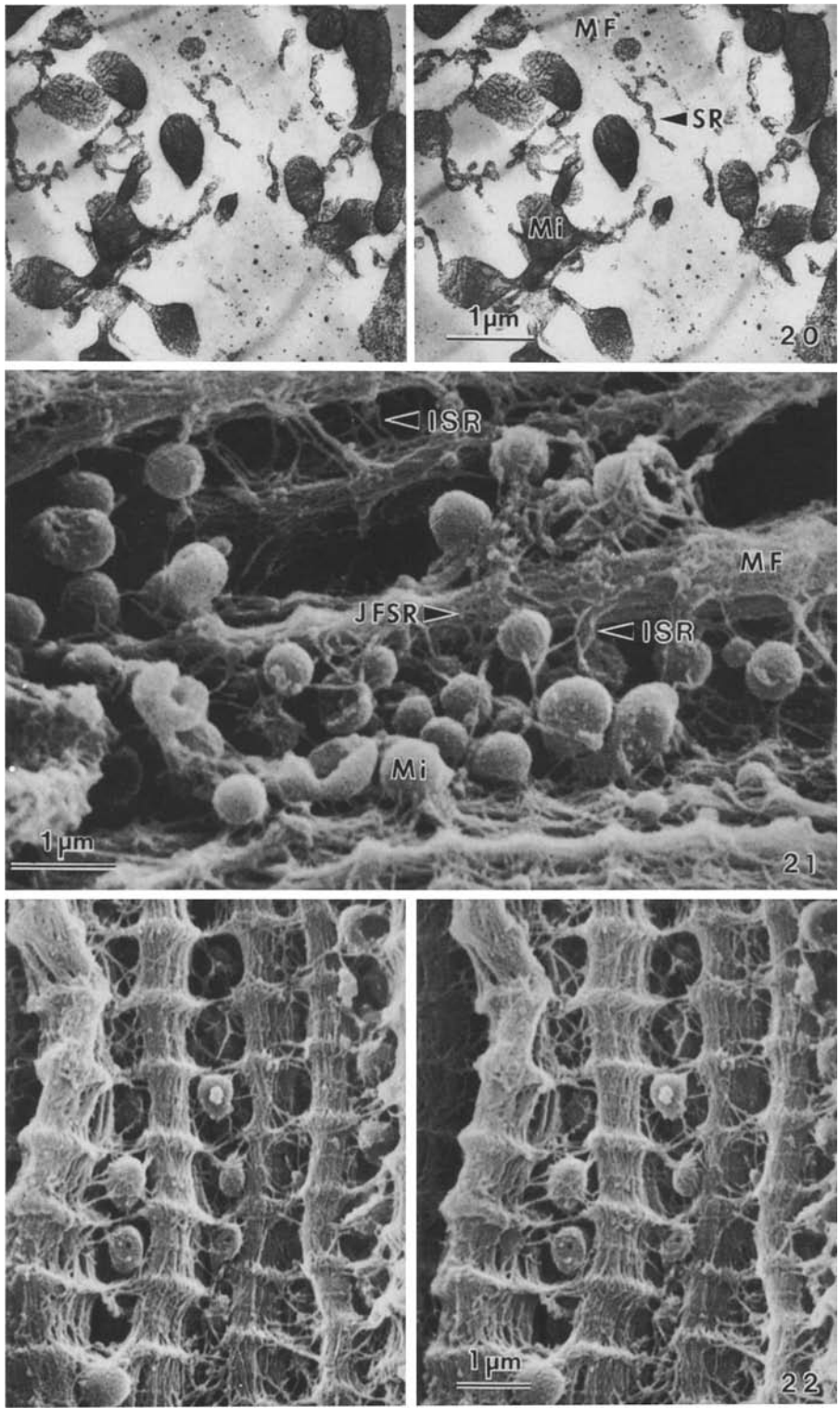

Fig. 20. A stereo-pair (12° tilt) transmission electron micrograph of a 1 μm thick section of Cu–Pb impregnated tissue demonstrating the three-dimensional relationship between SR and mitochondria (*Mi*). *MF*, myofibril. ×12800

Figs. 21–22. Mono (**Fig. 21**) and stereo-pair (12° tilt) (**Fig. 22**) scanning electron micrographs of cryofractured material. Note the strands of intermediary SR (*ISR*) spun out between mitochondria (*Mi*) and myofibrils (*MF*). These strands which are continous with the juxtafibrillar SR (*JFSR*), are preferentially branched off from the Z-band and M-band regions (**Fig. 22**). **Fig. 21**, ×15000; **Fig. 22**, ×10500

activities. Thus, it has been suggested by several authors that morphological and functional differences between the subsarcolemmal, interfibrillar and perinuclear mitochondria reflect their engagements as primary energy sources for different metabolic activities (Müller 1976; Palmer et al. 1977; Unverferth et al. 1981; Shimada et al. 1984).

The present study strongly indicates that the electron-dense submitochondrial particles of Cu–Pb impregnated material correspond to the parti-

culate structures exposed in freeze fractured mitochondria. If, indeed, these structures are identical, *en bloc* staining with a Cu–Pb citrate solution offers a new positive staining method for ultrastructural visualization of various proteins and respiratory enzymes associated with the mitochondrial membranes and cristae. In the past, however, the distribution of such submitochondrial macromolecules has been studied almost exclusively in freeze fractured material (Packer et al. 1974; Sjøstrand and Cassel 1978a, b; Sjøstrand 1983). Only the extrinsic portion of the ATP synthase complex has been identified successfully using a negative staining technique (Fernández-Morán et al. 1964; Racker et al. 1965).

Structures similar to the slender mitochondrial processes seen in the present material have been reported in normal myofibers of the cat papillary muscle (Fawcett and McNutt 1969), and in hypertrophied muscle cells of the human atrial tissue (Thiedemann and Ferrans 1977). The functional significance of these prolongations has not been entirely clarified. Fawcett and McNutt (1969) have suggested that the long and slender extensions are instrumental for the redistribution of the mitochondrial mass by penetrating the narrow interfibrillar clefts. In this way the diffusion distance from the main mitochondrial body to remote domains of the contractile material could be reduced. It also has been suggested that these prolongations represent a stage in mitochondrial proliferation (Fawcett and McNutt 1969), a view that is strongly favoured by the present investigation. It is well documented that new mitochondria arise from preexisting organelles by growth and subsequent division (Tandler et al. 1969; Attardi et al. 1975; Posakony et al. 1977). In this process the formation of internal septa appears to be the crucial factor promoting mitochondrial division. Examples of transverse septa subdividing the cardiac cell mitochondria have been observed in various animals under normal as well as experimental conditions (Onishi 1967; Tandler and Hoppel 1972; Publicover et al. 1977; Duncan et al. 1980). A morphometric study by Page et al. (1974) has shown that during normal postnatal growth the increase in the cumulative mitochondrial volume is due to the formation of additional mitochondria of the same size. Based on the present extensive TEM and SEM studies, it is resonable to conclude that the slender mitochondrial projections represent the initial stage in the formation of large and pleomorphic mitochondria. However, unequivocal evidence for the formation of internal septa bisecting the hypertrophied cardiac cell mitochondria has not been found in the present material or in the literature. Therefore, the extent to which and the mechanism by which the enlarged mitochondria may be subdivided into smaller, individual organelles, or may persist as large and pleomorphic organelles, remains to be elucidated.

It is well recognized that muscle contraction depends on a high degree of subcellular organization as well as on metabolic coordination between the energyproducing mitochondria and the Ca^{2+}-sequestering SR. Physical contact between the sarcotubular and outer mitochondrial membranes, manifested as interconnecting thread-like structures, has been reported in conventionally prepared myocardial cells of the gerbil (Dalen et al. 1983), mouse (Forbes and Sperelakis 1983) and man (Dalen et al. 1987b). These connections, denoted mito- reticular junctional fibers, to which an anchoring function has been attributed (Dalen et al. 1983), may be an integral part of the cytoskeletal system. SEM studies of the present cryofractured material have shown that strands of intermediary sarcotubules, predominately spun out from the juxtafibrillar SR at the Z- and M-band levels, make contacts with the surface of the interfibrillar mitochondria. The functional significance of this architectural arrangement remains unclear.

It has been shown here that, in the contact regions, some of the specifically contrasted transmembrane mitochondrial particles have fused with their sarcotubular counterparts. Morphologically these structures differ from the mito-reticular junctional fibers (Dalen et al. 1983, 1987b; Forbes and Sperelakis 1983). They may, however, correspond to the bridging particles between these two organelles that have been revealed in freeze fracture replicas of the dog myocardium (Scales 1981). Although the functional significance of such interconnecting structures remains obscure, it is tempting to suggest that they represent membrane-bound transport proteins which provide a direct interorganelle transport route for various metabolites and/or ions. It is also suggested that the observed fusion between the transmembrane particles of adjacent mitochondria represents a similar interorganelle communication system.

The metabolic function, if any, of the contact between specifically contrasted mitochondrial particles and nexus remains to be clarified. Strand-like interconnections between the nexuses and adjacent mitochondria have been reported in ventricular myocardial cells of other mammalian species (Forbes and Sperelakis 1982). According to the view of these authors, the close association between the two organelles may function as a mecha-

nism for buffering the intracellular Ca^{2+} concentration in regions adjacent to the nexuses, and thereby regulate the ionic transport through these intercellular junctions.

According to MacLennan and Holland (1975) most of the proteins embedded in the sarcotubular membrane consist of ATP driven Ca^{2+}-pumps. Therefore, it is conceivable that the majority of the selectively stained granular structures of the SR represent Ca^{2+}-pumps. Previously, these membrane components have been visualized in the TEM using negative staining or freeze fracture techniques (Ikemoto et al. 1968; Deamer and Baskin 1969; Sommer and Waugh 1976; Wang et al. 1979). The addition of tannic acid to the fixative has resulted in an asymmetrical contrasting of the SR membrane (Saito et al. 1978) corresponding to the asymmetric orientation of the Ca^{2+}-pumps shown by freeze fracture techniques (Packer et al. 1974; Scales and Inesi 1976; Wang et al. 1979).

Elucidation of the true metabolic functions of the ultrastructural findings in the present study must await further correlative ultrastructural and biochemical studies.

Acknowledgements. The author wish to express his sincere appreciation to Professor Paul Scheie, Texas Lutheran College, and Professor Thorvald Sætersdal., University of Bergen, for fruitful discussion and critical reading of the manuscript. The valuable technical assistance by Mr. Jakob Röli, Mrs. Anne Marie Sandsbakk Austarheim and Miss Brynhild Haugen is gratefully acknowledged. The biopsy material was kindly provided by Dr. Hogne Engedal, Department of Cardiac Surgery, Haukeland Hospital.

References

Attardi G, Costantino P, England J, Lynch D, Murphy W, Ojala D, Posakony J, Storrie B (1975) The biogenesis of mitochondria in HeLa cells: A molecular and cellular study. In: Birky CW, Perlman PS, Byers TJ (eds) Genetics and Biogenesis of Mitochondria and Chloroplasts. Ohio State University Press, Columbus, pp 3–65

Bugaisky L, Zak R (1986) Biological mechanisms of hypertrophy. In: Fozzard HA, Haber E, Jennings RB, Katz AM, Morgan HE (eds) The Heart and Cardiovascular System. Raven Press, New York, pp 1491–1506

Dalen H, Myklebust R, Sætersdal TS (1978) Cryofracture of paraffin-embedded heart muscle cells. J Microsc 112:139–151

Dalen H, Scheie P, Myklebust R, Sætersdal T (1983) An ultrastructural study of cryofractured myocardial cells with special attention to the relationship between mitochondria and sarcoplasmic reticulum. J Microsc 131:35–46

Dalen H, Sætersdal T, Ødegården S (1987a) Some ultrastructural features of the myocardial cells in the hypertrophied human papillary muscle. Virchows Arch [A] 410:281–294

Dalen H, Ødegården S, Sætersdal T (1987b) The application of various electron microscopic techniques for ultrastructural characterization of the human papillary heart muscle cell in biopsy material. Virchows Arch [A] 410:265–279

Deamer DW, Baskin RJ (1969) Ultrastructure of sarcoplasmic reticulum preparations. J Cell Biol 42:296–307

Ducan CJ, Greenaway HC, Publicover SJ, Rudge MF, Smith JL (1980) Experimental production of "septa" and apparent subdivision of muscle mitochondria. J Bioenerg Biomem 12:13–33

Echlin P (1975) Sputter coating techniques for scanning electron microscopy. Scan Elect Microsc I:217–224

Ericsson JLE, Brunk UT, Arborgh B (1978) Fixation. In: Johannessen JV (ed) Electron Microscopy in Human Medicine, vol 1, McGraw-Hill International Book Company, New York, pp 99–115

Fawcett DW, McNutt NS (1969) The ultrastructure of the cat myocardium. I. Ventricular papillary muscle. J Cell Biol 42:1–45

Fernández-Morán H, Oda T, Blair PV, Green DE (1964) A macromolecular repeating unit of mitochondrial structure and function. Correlated electron microscopic and biochemical studies of isolated mitochondria and submitochondrial particles of beef heart muscle. J Cell Biol 22:63–100

Ferrans VJ (1984) Cardiac hypertrophy: Morphological aspects. In: Zak R (ed) Growth of the Heart in Health and Disease. Raven Press, New York, pp 187–239

Forbes MS, Sperelakis N (1982) Association between gap junctions and mitochondria in mammalian myocardial cells. Tissue Cell 14:25–37

Forbes MS, Sperelakis N (1983) The membrane systems and cytoskeletal elements of mammalian myocardial cells. In: Dowben RM, Shay JW (eds) Cell and Muscle Motility, vol. 3. Plenum Publishing Corop, New York, pp 89–155

Hamrell BB, Alpert NR (1986) Cellular basis of the mechanical properties of hypertrophied myocardium. In: Fozzard HA, Haber E, Jennings RB, Katz AM, Morgan HE (eds) The Heart and Cardiovascular System. Raven Press, New York, pp 1507–1524

Ikemoto N, Sreter FA, Nakamura A, Gergely J (1968) Tryptic digestion and localization of calcium uptake and ATPase activity in fragments of sarcoplasmic reticulum. J Ultrastruct Res 23:216–232

Luft JH (1961) Improvements in epoxy resin embedding methods. J Biophys Biochem Cytol 9:409–414

MacLennan DH, Holland PC (1975) Calcium transport in sarcoplasmic reticulum. Annu Rev Biophys Bioeng 4:377–404

Müller W (1976) Subsarcolemmal mitochondria and capillarization of soleus muscle fibers in young rats subjected to an endurance training. A morphometric study of semithin sections. Cell Tiss Res 174:367–389

Onishi S (1967) Die Feinstruktur des Herzmuskels nach Aderlaß bei der Ratte. Zugleich ein Beitrag zur Teilung und Vermehrung von Herzmuskelmitochondrien. Beitr Path Anat 136:96–132

Packer L, Mehard CW, Meissner G, Zahler WL, Fleischer S (1974) The structural role of lipids in mitochondrial and sarcoplasmic reticulum membranes. Freeze-fracture electron microscopy studies. Biochem Biophys Acta 363:159–181

Page E, Earley J, Power B (1974) Normal growth of ultrastructures in rat left ventricular myocardial cells. Circulation Res 34 & 35 (Suppl II) II 12-II 16

Palmer JW, Tandler B, Hoppel CL (1977) Biochemical properties of subsarcolemmal and interfibrillar mitochondria isolated from rat cardiac muscle. J Biol Chem 252:8731–8739

Posakony JW, England JM, Attardi G (1977) Mitochondrial growth and division during the cell cycle in HeLa cells. J Cell Biol 74:468–491

Publicover SJ, Duncan CJ, Smith JL (1977) Ultrastructural changes in muscle mitochondria *in situ*, including the appar-

ent development of internal septa, associated with the uptake and release of calcium. Cell Tiss Res 185:373–385
Racker E, Tyler DD, Eastbrook RW, Conover TE, Parsons DF, Chance B (1965) Correlations between electron-transport activity, ATPase, and morphology of submitochondrial particles. In: King TE, Mason HS, Morrison M (eds) Oxidases and Related Redox Systems, John Wiley and Sons Inc, New York, pp 1077–1094
Reynolds ES (1963) The use of lead citrate at high pH as an electron-opaque stain in electron microscopy. J Cell Biol 17:208–212
Saito A, Wang C-T, Fleischer S (1978) Membrane asymmetry and enhanced ultrastructural detail of sarcoplasmic reticulum revealed with use of tannic acid. J Cell Biol 79:601–616
Scales DJ (1981) Aspects of the mammalian cardiac sarcotubular system revealed by freeze fracture electron microscopy. J Mol Cell Cardiol 13:373–380
Scales D, Inesi G (1976) Assembly of ATPase protein in sarcoplasmic reticulum membranes. Biophys J 16:735–751
Segretain D, Rambourg A, Clermont Y (1981) Three dimensional arrangement of mitochondria and endoplasmic reticulum in the heart muscle fiber of the rat. Anat Rec 200:139–151
Shimada T, Horita K, Murakami M, Ogura R (1984) Morphological studies of different mitochondrial populations in monkey myocardial cells. Cell Tissue Res 238:577–582
Sjøstrand FS (1983) The diversity of function and structure of cellular membranes. In: Roodyn DB (ed) Subcellular Biochemistry, vol 9, Plenum Press, New York, pp 335–393
Sjøstrand FS, Cassel RZ (1978a) Structure of inner membranes in rat heart muscle mitochondria as revealed by means of freeze-fracturing. J Ultrastruct Res 63:111–137
Sjøstrand FS, Cassel RZ (1978b) The structure of the surface membranes in rat heart muscle mitochondria as revealed by freeze-fracturing. J Ultrastruct Res 63:138–154
Sommer JR, Waugh RA (1976) The ultrastructure of the mammalian cardiac muscle cell – With special emphasis on the tubular membrane systems. A review. Am J Pathol 82:192–232
Tandler B, Erlandson RA, Smith AL, Wynder EL (1969) Riboflavin and mouse hepatic cell structure and function. II. Division of mitochondria during recovery from simple deficiency. J Cell Biol 41:477–493
Tandler B, Hoppel CL (1972) Possible division of cardiac mitochondria. Anat Rec 173:309–323
Thiedemann K-U, Ferrans VJ (1977) Left atrial ultrastructure in mitral valvular disease. Am J Pathol 89:575–604
Thiéry G, Bergeron M (1976) Morphologie spatiale des mitochondries des tubes proximaux et distaux du néphron. Rev Can Biol 35:211–216
Unverferth DV, Leier CV, Brierley GP, Magorien RD, Baba N (1981) Human myocardial mitochondria: Size differences in parts of the cell. Exp Mol Pathol 35:184–188
Wang C-T, Saito A, Fleischer S (1979) Correlation of ultrastructure of reconstituted sarcoplasmic reticulum membrane vesicles with variation in phospholipid to protein ratio. J Biol Chem 254:9209–9219
Watson ML (1958) Staining of tissue sections for electron microscopy with heavy metals. J Biophys Biochem Cytol 4:475–479

Received June 30, 1988 / Accepted November 11, 1988